



## Diffusion Boundary Layer Studies in an Industrial Wafer Plating Cell

B. Q. Wu,<sup>\*z</sup> Z. Liu,<sup>\*</sup> A. Keigler, and J. Harrell

Nexx Systems, Billerica, Massachusetts 01821-3904, USA

Linear sweep voltammetry and chronoamperometry methods were used to measure limiting current in an industrial wafer-plating cell. Copper deposition in a dilute solution, under mass-transfer-limited conditions, is used to study the variation of the mass transfer boundary-layer thickness. It is shown that a shear-plate fluid agitation mechanism is capable of generating a thin (*i.e.*,  $<10 \mu\text{m}$ ), spatially uniform and nonperiodic boundary layer across the entire wafer. It is anticipated that thin boundary layer deposition will prove to be beneficial in MEMS, flip-chip bumping, and WL-CSP applications.  
© 2005 The Electrochemical Society. [DOI: 10.1149/1.1874674] All rights reserved.

Manuscript submitted August 5, 2004; revised manuscript received November 23, 2004. Available electronically March 25, 2005.

A thin, uniform, and stationary diffusion boundary layer is important in obtaining high-quality electrodeposits. Limiting current depends on thickness of the diffusion boundary layer for a given reactant concentration. Plating current is then usually set below one-half of limiting current to obtain plated deposits acceptable for their appearance and uniformity. In cases where operating current is set to greater than one-half of limiting current, the effects of mass transfer typically impact the morphology of the deposit, and rough growth is often observed. Moreover, control of limiting current density and diffusion boundary layer thickness becomes even more important when the subject is the plating of metal alloys. In alloy deposition, cell potential is set such that one metal is deposited at its diffusion limiting current. Thus, uniformity of the diffusion boundary layer significantly influences composition of the final plated alloy, and its material properties.

The reciprocating paddle cell is a known practical method for depositing alloy films on wafer substrates. It has been shown that the diffusion boundary layer's thickness profile, in a paddle-cell, may be periodic in nature due to the wake trailing the paddle.<sup>1</sup> It has also been shown that paddle distance from the cathode has a greater impact on deposition uniformity than does paddle speed.<sup>2</sup>

The primary electrochemical technique for measurement of the mass transfer boundary-layer thickness is determination of limiting current. At limiting current, concentration of reacting species is virtually zero over the entire electrode surface. Limiting current measurements are usually carried out in a traditional three-electrode cell, using a potentiostat. Techniques for determining limiting current and mass-transfer coefficient correlation, for a variety of different electrode geometries and fluid flow conditions in laboratory experimental cells, were reviewed by Selman and Tobias.<sup>3</sup> However, only limited methods have been available to characterize the mass transfer boundary layer in industrial wafer plating cells, due to their complicated cell geometries and limited accesses for probes. It is difficult to install a standard reference electrode in an industrial wafer plating cell. Moreover, a potentiostat is not usually available in a typical wafer fabrication facility. These problems are barriers to transferring experimental results obtained from bench- or beaker-scale testing to wafer-scale industrial plating tools.

In this study, linear sweep voltammetry and chronoamperometry methods were used to measure limiting current in a dilute solution in a fully operational industrial wafer plating cell. Copper deposition in a dilute solution, under mass-transfer-limited conditions, was used to study the spatial and temporal variation of the mass transfer diffusion layer thickness on wafers. Deposition of Cu in a dilute solution under mass-transfer-limited conditions was originally presented by Schwartz<sup>1</sup> and Powers<sup>4</sup> to study cathodic mass transfer in an electrochemical cell. The principal advantage of this technique is

that it requires neither a potentiostat nor a regular reference electrode; thus it is practical to apply this method to many industrial plating and etching processes.

### Experimental

Experiments were performed on a NEXX Systems' Stratus plating cell, equipped with a shear plate fluid agitator, designed to promote mass transfer for MEMS, flip-chip bumping, and WL-CSP applications. Motion of the plate is parallel to the cathode, at a distance of less than 2 mm from the wafer surface. The shear plate has an array of slots through it such that the edges of the slots cause fluid mixing as the shear plate are reciprocated parallel to the cathode. Shear flow is generated on the surface of the cathode, reducing boundary layer thickness. Because the copper damascene process is dominated by diffusion of copper ions in a submicron trench or via, the shear flow may not have a big impact on the filling process.

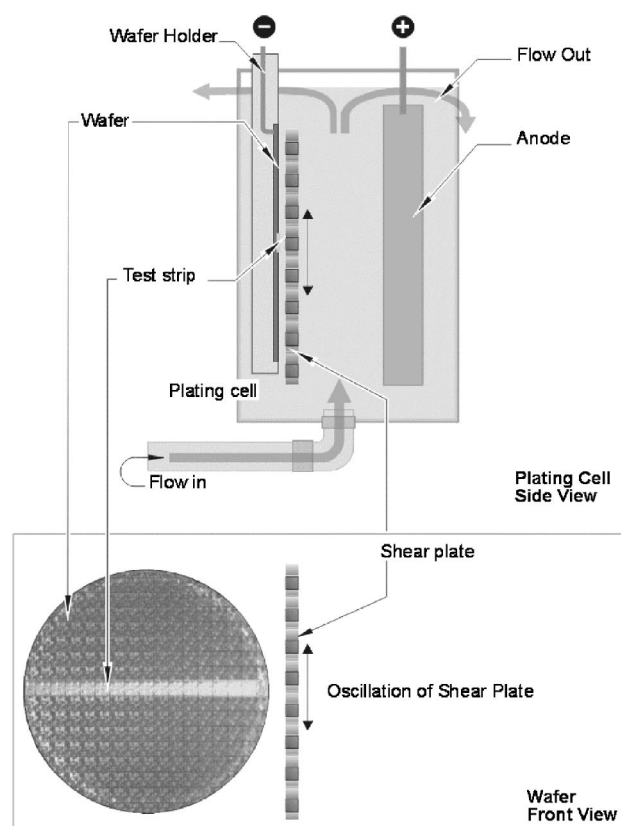


Figure 1. (top) Schematic cross section of shear plate in plating cell; (bottom) wafer sample.

\* Electrochemical Society Active Member.

<sup>z</sup> E-mail: Bill\_wu@nexxsystems.com

**Table I. Composition of test solution.**

CuSO <sub>4</sub> · 5H <sub>2</sub> O	H <sub>2</sub> SO <sub>4</sub>	HCl
2.4 g/L	90 g/L	1.2 ppm

However, the shear flow may be beneficial for uniformly distributing additives crossing the entire wafer and reducing overplate. A schematic cross-section of the cell used in our experiments is shown in Fig. 1. Uniform and accurate reciprocating motion of the shear plate is driven by a computer-controlled linear motor. The stroke length of the shear plate is 2-4 cm. The test of the reciprocating paddle was performed in the same process cell, where a paddle arm replaced the shear plate.

Electrolyte was continuously recirculated through the cell from a surrounding reservoir, throughout the experiment. Bath turnover rate was 0.8 min, at a flow rate of 7.3 GPM (27.6 L/min).

The chemistry for measuring the limiting current is listed in Table I. Note that a dilute solution for measuring cathode limiting current creates a situation at the cathode wherein mass transfer control occurs at a low current, below 50 mA, thereby reducing possible variation in electrical potential at the anode.

The anode was a solid copper disk with an exposed area of 300 cm<sup>2</sup>. An important aspect of our experimental method is that the anode functions as both the reference and counter electrodes. To this end, overpotential at the anode must be adjusted to the lowest possible value by selecting proper experimental conditions.

Overpotential,  $\eta_s$ , of the anode can be approximated by a linear expression from the Butler-Volmer equation at low current density

$$\eta_s = \frac{i}{i_o} \frac{RT}{(\alpha_a + \alpha_c)2F} \quad [1]$$

The sum of transfer coefficients,  $\alpha_a + \alpha_c$ , has a theoretical value of 2. The exchange current density,  $i_o$ , can be expressed as<sup>5</sup>

$$i_o = \left( \frac{C_{Cu^{2+}}}{C_{Cu^{2+}}^\infty} \right)^\gamma i_{o}(C_{Cu^{2+}}^\infty) \quad [2]$$

Assuming  $\gamma = 0.6$ , and taking  $i_o$  equal to 1 mA/cm<sup>2</sup> for a cupric ion concentration of 0.1 molar,<sup>6</sup> then  $i_o$  for the test solution is  $\sim 0.2$  mA/cm<sup>2</sup>. Therefore, a 40 mA current would generate overpotential of 4.3 mV at the anode, small enough to ensure the anode can act as a reference electrode for limiting current measurements. A

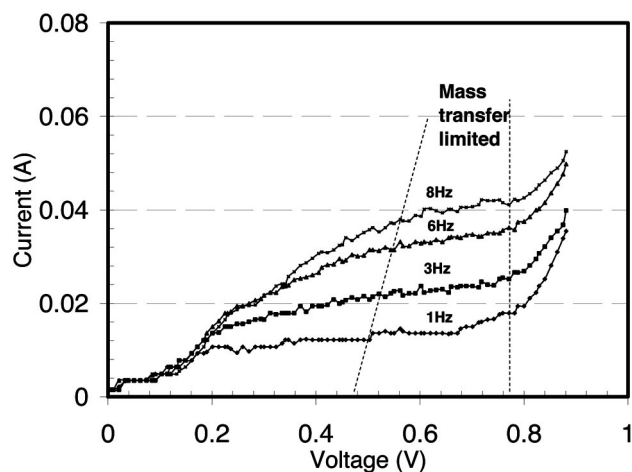


**Figure 2.** Typical current vs. cell voltage curves obtained from sheet wafer experiments, showing the Cu<sup>2+</sup> mass-transfer-limited regime. Different limiting currents correspond to different shear plate agitation frequencies.

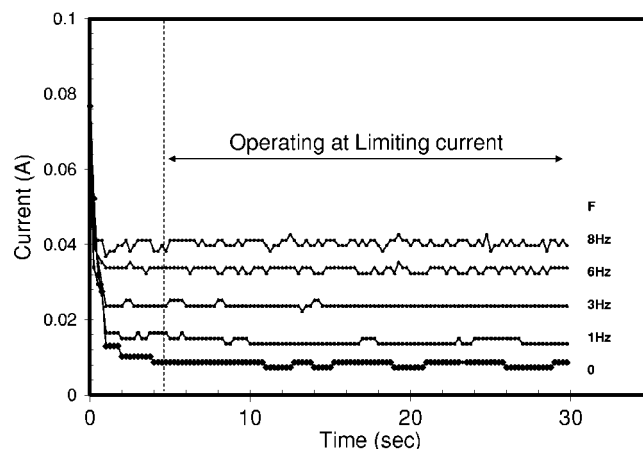


**Figure 3.** Typical response current curves obtained in sheet wafer experiments at a constant cell voltage (0.65 V). Various shear plate agitation frequencies in the mass-transfer-limited regime are shown.

small exposed surface area of the cathode was used to produce a small limiting current; this in turn generates a small current density and low overpotential on the anode.

Two substrate types, uniform flat copper seed layer wafers and photoresist patterned wafers, were selected for limiting current testing. The seed layer cathodes were 200 mm silicon wafers with a 1000 Å sputtered copper seed layer. The wafers were masked to expose a narrow band across the wafer diameter, 5 cm<sup>2</sup> in total area. The patterned wafer also was a 200 mm wafer masked to expose a band across its diameter; the band width was adjusted to a total exposed area of 5 cm<sup>2</sup>. The exposed band was perpendicular to the direction of shear plate oscillation.

Both morphology and uniformity tests were carried out on patterned wafers. Patterned wafers had a plateable area of 57.37 cm<sup>2</sup>. They were patterned with bump arrays of  $\sim 50$   $\mu$ m thick photoresist on 1000 Å Cu-seed layer. Each die was structured with a pattern of 39  $\times$  39 bumps of  $\sim 130$   $\mu$ m diam, arrayed on  $\sim 250$   $\mu$ m pitch. Streets 500  $\mu$ m wide absent of bump openings separated individual die. Wafers were uniformly populated out to an edge exclusion zone  $\sim 3$   $\mu$ m. Thickness of bumps was measured on a Tencor P12 automated scanning profilometer. On-wafer uniformity (one sigma), was measured and evaluated across a row of bumps within a wafer.

An HP 6632A plating power supply was used to measure cathode limiting current. The dynamic polarization curve was obtained using a linear voltage sweep method. Cell voltage was scanned from 0 to 1.0 V at a scan rate of 10 mV/s (see Fig. 2). A wide and flat limiting current plateau, corresponding to the mass-transfer-limited regime,

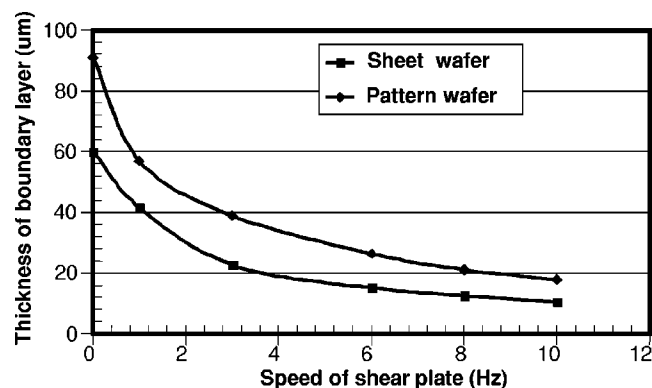


**Figure 4.** Effect of shear plate speed on measured thickness of the mass transfer boundary layer.

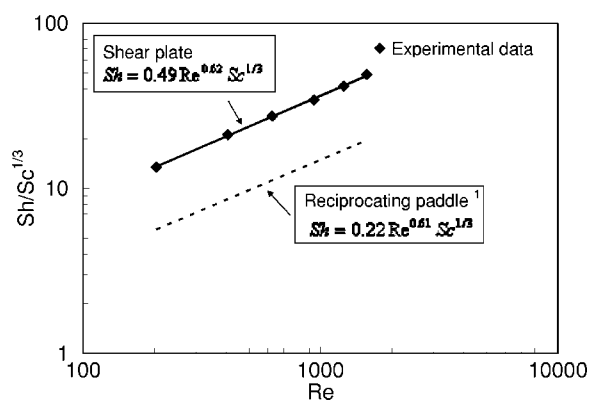


**Figure 5.** Comparison of mass-transfer correlations between the shear plate and a reciprocating paddle.

was observed on polarization curves. Although surface area of the substrate was smooth prior to testing, we expected surface area of the cathode to increase with the development of surface roughness during scan. To precisely measure the limiting current, a constant cell voltage within the mass-transfer-limited region, was applied. Response of cell current was then recorded (see Fig. 3). The minimum data interval was 0.25 s that is limited by the power supply system. Within 2 s, limiting current was reached and thereafter remained fairly constant. Each test was carried out on a fresh surface. The limiting current was determined by time-averaging. A standard deviation for the limiting current was also calculated.

With a known concentration of  $\text{Cu}^{2+}$  ions in the solution and limiting current, we obtain the Nernst diffusion layer thickness  $\delta$

$$\delta = nF \frac{D_{\text{Cu}^{2+}} C_b}{i_l} \quad [3]$$

where  $n$  is charge number,  $F$  is Faraday constant,  $D$  is diffusivity of  $\text{Cu}^{2+}$ ,  $C_b$  is bulk concentration of copper ion, and  $\delta$  is thickness of the boundary layer. Effect of migration on the limiting current was presumed negligible due to high concentration of support electrolyte.<sup>7</sup> The diffusivity of  $\text{Cu}^{2+}$  was taken to be  $5.37 \times 10^{-6} \text{ cm}^2/\text{s}$ .<sup>8</sup>

At mass-transfer limiting condition, the mass-transfer coefficient can be expressed as

$$\kappa = \frac{i_l}{nFC_b} \quad [4]$$

Therefore, the diffusion layer thickness in Eq. 3 may be expressed in terms of the mass-transfer coefficient and the diffusivity of cupric ions

$$\delta = \frac{D_{\text{Cu}^{2+}}}{\kappa} \quad [5]$$

With a known limiting current, the  $\kappa$  could be determined. The mass-transfer coefficient is related to the fluid dynamics in the cell from dimensional analysis by a characteristic velocity and characteristic mixing length. Based on the results<sup>1,2</sup> of mass transfer stud-

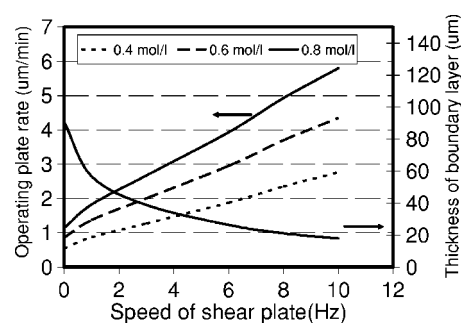


**Figure 6.** Estimated plating rate, based on cathode limiting current vs. shear plate speed with various concentration of cupric ions. Computed for patterned wafers with 50  $\mu\text{m}$  thick photoresist and 130  $\mu\text{m}$  via diameter.

ies from reciprocating paddle cells, the line shear plate velocity ( $U$ ) and shear plate mixing length ( $L$ ), which equal shear plate height above the cathode surface plus thickness of the shear plate, are expected to be related by

$$Sh = aRe^b Sc^{1/3} \quad [6]$$

where  $Sh = \kappa L/D$  is the Sherwood number,  $Re = UL/\nu$  is the Reynolds number,  $Sc = \nu/D$  is the Schmidt number, and  $\nu$  is kinematic viscosity of the fluid. The Schmidt number was 2147 for the test solution in this study.

## Results and Discussion

**Thickness of boundary layer.**—The speed of the shear plate had a significant impact on the cathode limiting current (see Fig. 3 and 4). A six-fold larger limiting current was achieved using a shear plate vs. using a 28 LPM flow across the sheet wafer without agitation at the cathode. The effective boundary layer thickness is estimated to be near 10  $\mu\text{m}$  at a shear plate reciprocation frequency of 10 Hz.

To determine the coefficients in Eq. 6, a plot of  $Sh/Sc^{1/3}$  vs.  $Re$  is given in Fig. 5. Coefficient  $a = 0.49$  and coefficient  $b = 0.62$ . The mass-transfer correlation of the form in Eq. 6 then becomes

$$Sh = 0.49Re^{0.62} Sc^{1/3} \quad [7]$$

This result is similar to mass-transfer correlation obtained from a commercial reciprocating agitation system with a paddle consisting of a pair of separated and opposing triangular blocks parallel to the cathode surface<sup>1</sup>

$$Sh = 0.22Re^{0.61} Sc^{1/3} \quad [8]$$

The correlation of Eq. 8 was plotted and compared with Eq. 7 in Fig. 5 by using the same characteristic variables. In comparison to reciprocating paddle agitation, the shear plate shows a higher Sherwood number (almost double coefficient  $a$ ) indicating a higher mass-transfer rate for the range of Reynolds number studied.

On patterned wafers with 50  $\mu\text{m}$  thick photoresist, the shear plate generated an effective boundary layer thickness of 20  $\mu\text{m}$  at the upper end of the shear plate frequency. The trenches on photoresist patterned wafer are in the range of 10 to 100  $\mu\text{m}$ , a scale that is

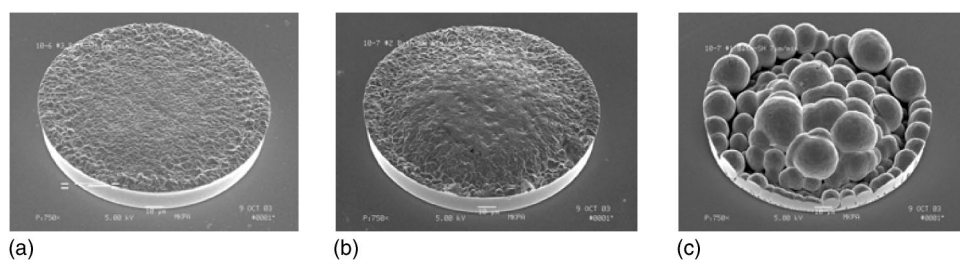


**Figure 7.** Effect of mass transfer on bump shape in Shipley InterVia 8502/8540 copper bath, (a) 5  $\mu\text{m}/\text{min}$ , 6 Hz,  $i/i_L = 0.6$ ; (b) 6  $\mu\text{m}/\text{min}$ , 6 Hz,  $i/i_L = 0.8$ ; (c) 7  $\mu\text{m}/\text{min}$ , 6 Hz,  $i/i_L = 1.0$

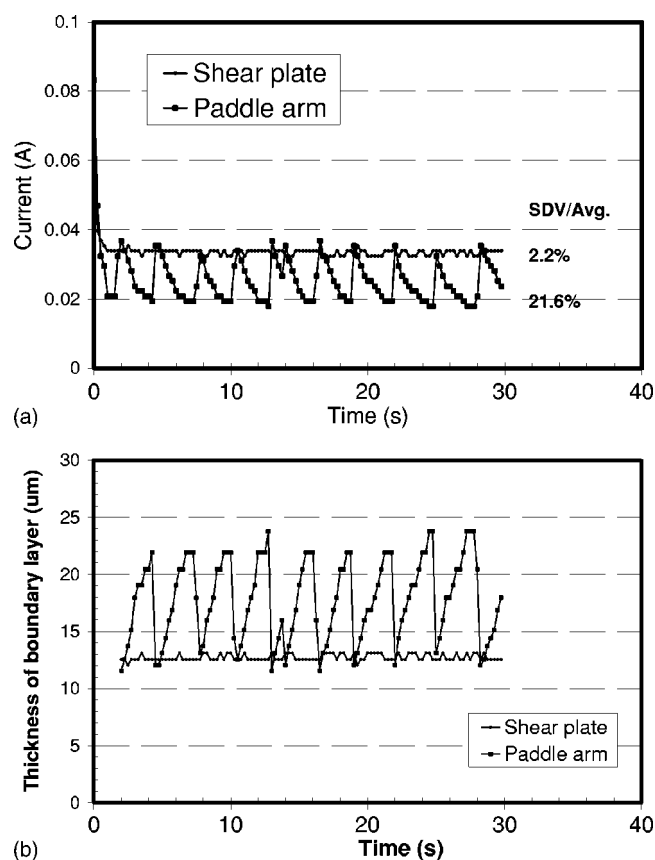


**Figure 8.** Comparison of time dependent behaviors of single blade paddle arm and shear plate on (a) limiting current and (b) thickness of boundary layer, at 24 cm/s of speed on the sheet wafer.

influenced by convection.<sup>9</sup> If we adopt Debecker's definition of the Peclet number ( $Pe$ ), where  $L$  is diameter of the trench, the paddle speed is  $U_o$ , and  $B$  is distance between the electrodes<sup>10</sup>

$$Pe = \left( \frac{U_o L}{B} \right) \frac{L}{D} \quad [9]$$

then at a paddle speed of 20 cm/s, the Peclet number would be 50, indicating that convection plays a role in controlling the deposition rate. At a Peclet number of 100, the process would be convection dominated. Obviously, the wake trailing of the body of the shear plate's cross members is able to penetrate deep into the trench on the patterned wafers.

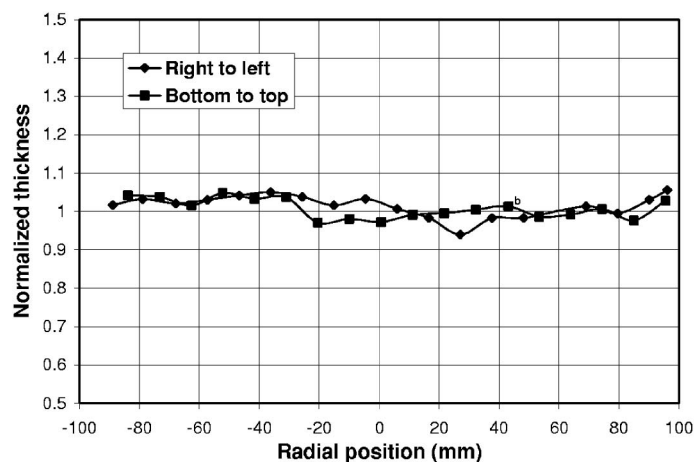


**Figure 9.** Normalized thicknesses of Cu pattern deposition under mass-transfer-limited conditions. Normalized thickness = thickness/wafer-mean thickness; 6 Hz shear plate oscillation frequency, 0.7 V cell voltage,  $\sim 4.5$  ma/cm<sup>2</sup> average current density.

The limiting current depends on  $Cu^{2+}$  concentration and fluid dynamic conditions. With a fixed thickness of the boundary layer, the cathode limiting current increases with increasing  $Cu^{2+}$  concentration. Using the thickness of the diffusion boundary layer corresponding to shear plate speed derived and measured as above (Fig. 4), the limiting current in commercial copper plating baths can be estimated using Eq. 3. To obtain plated deposits of acceptable appearance and uniformity, the practical operating current should be set below one-half of cathode limiting current.

With these considerations in mind, deposition rates on patterned wafers vs. speed of the shear plate for various  $Cu^{2+}$  concentrations are plotted in Fig. 6, where operating plating current was set at one-half of limiting current. For comparison, 0.4, 0.6, and 0.8 mol/L of the  $Cu^{2+}$  concentration in the baths were selected.

At relatively high shear plate speeds, a deposition rate of  $\sim 2$  -  $6$   $\mu\text{m}/\text{min}$  is achievable for through-mask copper deposition on patterned wafers using commercially available copper baths. For instance, with shear plate speed set to 6 Hz, then a smooth, flat bump shape is obtained at a deposition rate of  $4.0$   $\mu\text{m}/\text{min}$  in the 0.8 mol/L bath.

To confirm our estimated deposition rates in Fig. 6, we plated patterned wafers in Shipley InterVia 8502/8540 copper bath, following which their bump shape was imaged by SEM. Figure 7 shows the effects of mass transfer on bump shape on patterned wafers.

At a shear plate oscillation frequency of 6 Hz, and a ratio of operating current to limiting current of 0.6, the Cu bumps are flat at a plating rate of  $5$   $\mu\text{m}/\text{min}$  (Fig. 7a). Hence, as a result of the influence of the shear plate, a fairly smooth deposit was obtained at this relatively high current density. A uniform surface of bumps obtained near limiting current is also consistent with results of DeBecker *et al.*,<sup>10</sup> who shows that more uniform current distribution is obtained by periodic flow than by unidirectional flow.

When the deposition rate was increased to  $6$   $\mu\text{m}/\text{min}$ , mass transfer limitations started to play a role. The bump grows at a faster rate in the center due to greater agitation (Fig. 7b). The bump growth at the extreme edge is consistent with observations by Kondo *et al.*<sup>11</sup>

With further increase in plating rate to  $7$   $\mu\text{m}/\text{min}$ , representing a ratio of operating current to limiting current of 1.0, the deposition becomes nearly mass transfer controlled and a nodular growth is observed (Fig. 7c). SEM images of bump shape at various deposition rates are consistent with predictions from Fig. 6.

*Time dependence of boundary layer.*—Chronoamperometry curves can also be used to monitor the time-dependent behavior of limiting current. As shown in Fig. 8, the variation of limiting current is only around 2% (one sigma) over the range of shear plate oscillation frequencies from 3 to 8 Hz. This indicates that the shear plate provides a stable limiting current. It has been shown that for conventional paddle arm cells, agitation likely arises due to vortices shed from the paddle that are  $90^\circ$  out of phase with the paddle

motion.<sup>1</sup> For a single paddle with a stroke length across the whole wafer, the limiting current will be periodic in nature with about 21.6% variation in one sigma (see Fig. 8a). With the shear plate, an array vortex line that moves across the cathode surface with rapid periodic motion creates a uniform diffusion boundary layer by enhancing uniformity intensity of vortex mixing.<sup>10</sup> By using the above calculation to convert the limiting currents into the boundary layer thickness; the time-dependence of the boundary layer is shown in Fig. 8b. It can be observed from this data that the boundary layer is periodic for a single paddle and relatively constant for the shear plate agitation.

*Spatial dependence of boundary layer.*—To further investigate uniformity of the diffusion boundary layer across the whole wafer surface, a patterned wafer was plated under limited current in the dilute solution. To reduce measurement errors caused by rough growth under this mass-transfer-limited condition, a normal additive package of commercial bright copper bath was added to the dilute electrolyte. A smooth surface was obtained with bumps of  $\sim 250$  Armstrong average roughnesses. Figure 9 shows bump height distribution across a wafer from bottom to top and from left to right. Because the deposit is obtained at diffusion limited, individual bumps have a domed top surface so that the thickness measurement is noising. However, the distribution of thickness across the wafer is flat and shows no radial or pattern to the boundary layer thickness. This demonstrates that the shear plate design is capable of generating a thin and uniform “blanket” mass transfer boundary layer over the entire wafer.

### Conclusion

This study employed several methods to study the mass transfer boundary layer within an industrial wafer plating cell. Linear sweep voltammetry and chronoamperometry methods were used to mea-

sure limiting current. Copper deposition, under limiting current conditions in a dilute solution, is a useful tool for characterizing the distribution of the mass transfer diffusion layer both spatially and temporally. We report that a novel fluid agitation shear plate that is capable of generating a thin, uniform, and nonperiodic boundary layer across the entire wafer surface which would be beneficial for MEMS, flip-chip bumping, and WL-CSP applications.

### Acknowledgments

The authors thank Professor D. Barkey of the University of New Hampshire for his review and comment. The authors also thank R. Liu for providing assistance on the experimental measurements and J. Drexler for editing the paper.

*Nexx Systems assisted in meeting the publication costs of this article.*

### References

1. D. T. Schwartz, B. G. Higgins, P. Stroeve, and D. Borowski, *J. Electrochem. Soc.*, **134**, 1639 (1987).
2. D. E. Rice, D. Sundstrom, M. F. McEachern, L. A. Klumb, and J. B. Talbot, *J. Electrochem. Soc.*, **135**, 2777 (1988).
3. J. R. Selman and C. W. Tobias, in *Advances in Chemical Engineering*, T. Drew, Editor, p. 211, Academic Press, New York (1978).
4. J. V. Powers and L. T. Romankiw, U.S. Pat. 3,652,442 (1972).
5. E. Mattsson and J. O'M. Bockris, *Trans. Faraday Soc.*, **55**, 1586 (1959).
6. J. Newman, in *Electrochemical Systems*, Prentice-Hall, Englewood Cliffs, NJ (1988).
7. B. Pillary and J. Newman, *J. Electrochem. Soc.*, **140**, 414 (1993).
8. J. T. Hinatsu and F. R. Foulkes, *J. Electrochem. Soc.*, **136**, 125 (1989).
9. D. P. Barkey, in *Advances in Electrochemical Science and Engineering*, R. C. Alkire and D. M. Kolb, Editors, Wiley-VCH, Weinheim (2002).
10. B. DeBecker, D. Yang, P. F. Doby, V. Modi, and A. C. West, *J. Electrochem. Soc.*, **142**, 3413 (1995).
11. K. Kondo, K. Fukui, K. Uno, and K. Shinhara, *J. Electrochem. Soc.*, **143**, 1880 (1996).